

## Loss of Control in Flight Diagnostics

V.I. Akhrameev<sup>1\*</sup>, A.G. Kostylev<sup>2</sup>, D.V.Plaksin<sup>2</sup>, V.N. Shvakin<sup>3</sup>

<sup>1</sup>Moscow Institute of Physics and Technology, Dolgoprudny, Moscow Region, Russian Federation.

<sup>2</sup>State University of Civil Aviation, Saint-Petersburg, Russian Federation.

<sup>3</sup>The Federal Agency for Air Transport (Rosaviatsiya), Moscow, Russian Federation.

### Abstract:

As a follow-up to the article titled Critical Flight Conditions at High Angles of Attack, Related to Loss of Control in Lateral Motion (Advances in Military Technology, Vol. 11, No. 1, June 2016), which deals with the issue of detecting critical flight conditions, this article considers the issue of ensuring the safety of light aircraft flights and protecting light aircraft from atmospheric disturbances which are caused by large-scale turbulence or trailing vortices from other aircraft. At low altitudes, this becomes an issue of particular concern if the final approach is made without using a weather radar and in low visibility conditions. The article analyzes the differences between airplane and helicopter trailing vortices and discusses the danger from downbursts. It suggests algorithms for determining the conditions under which an aircraft will fly into a downburst and methods of handling this dangerous situation using such on-board tools as the aircraft computer and the LCD display. It also discusses the results of experiments conducted to test the proposed algorithms and methods. The experiments were carried out using the Sigma-Classic flight simulator with a take-off weight of 540 kg. The article also suggests an approach to the selection of principles and methods used by the algorithms of the aircraft computer in flight risk assessment and decision support.

**Publication History:** Received: 02 November 2018 | Revised: 07 December 2018 | Accepted: 12 December 2018

### Keywords:

flight safety, sudden and unexpected changes in flight conditions, stalling, loss of control in-flight (upset), large-scale atmospheric turbulence, downburst, aircraft trailing vortex, helicopter trailing vortex, system algorithms in aircraft, display algorithms, ground testing, flight simulator testing, final approach safety, decision support.

## INTRODUCTION

According to statistics for accidents in civil aviation which have been collected over the past three decades, the share of accidents caused by aircraft failures has significantly decreased (it currently amounts to 10-15%), while human factors have become the main cause of accidents in civil aviation [1-5], with their share amounting to 85-90%. At the same time, in the overwhelming majority of cases (see. Fig. 1) there are only two causes of air crashes, which are Loss of Control In-Flight (LOC-I) and Controlled Flight Into Terrain (CFIT).

The latter one used to be the main cause of air crashes until a requirement was made that all aircraft had to be equipped with ground proximity warning modules (EGPWS, TAWS).

“After that, in the first decade of the new century the number of such incidents (CFIT) began to decline, while the number of disasters due to Loss of Control in Flight(LOC-I) increased,” –

says Dr. Sunjoo Advani, President of International Committee for Aviation Training in Extended Envelopes (ICATEE) created by Royal Aeronautical Society (RAeS).

“Loss of control most often occurs as a result of stalling. Pilots are well prepared, planes are equipped with stall protection systems, but accidents still happen. Why?” – Dr. Sunjoo Advani ponders and suggests an answer. “Because loss of control in-flight is a rare and unpredictable phenomenon which may have disastrous consequences. It is very difficult to prepare pilots for handling such a situation, and the existing pilot training programs do not address this challenge.”

Loss of Control In-Flight (LOC-I), which may result in upset and stall, was chosen by ICAO as a focus area to improve safety (paragraph 3.1.3 of ICAO Doc 10004 “2017-2019 Global Aviation Safety Plan”). Preventing accidents associated with Loss of Control In-Flight is a complex task. In order to

\*Address correspondence to this author at Moscow Institute of Physics and Technology (State University), Dolgoprudny, Moscow Region, Russian Federation.; E-mail: akhrameev\_vi@mail.ru

### Mesford Publisher Inc

Office Address: Suite 2205, 350 Webb Drive, Mississauga, ON L5B3W4, Canada; T: +1 (647) 7109849 | E: caic@mesford.ca, contact@mesford.ca, <https://mesford.ca/journals/caic/>

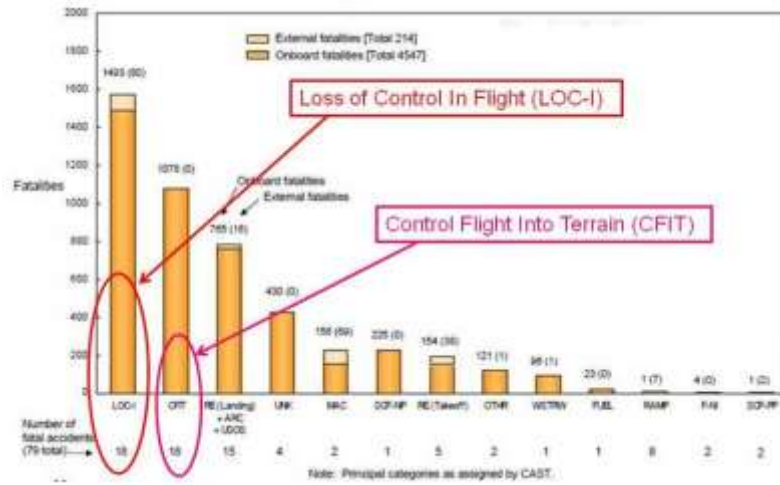


Fig. (1). Causes of aviation accidents in civil aviation.

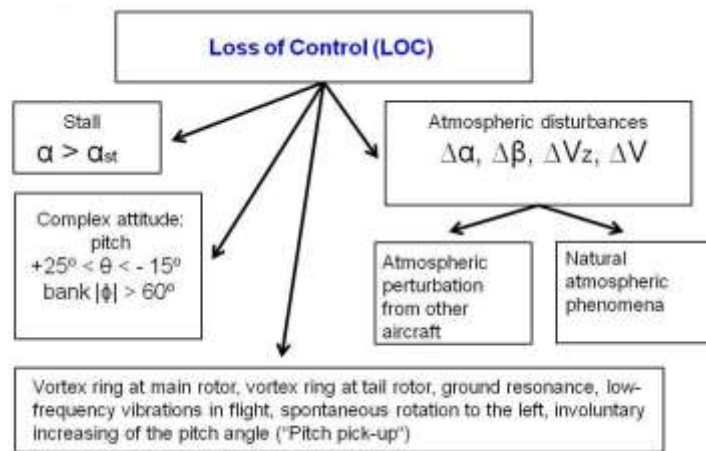


Fig. (2). The main causes of atmospheric disturbances.

solve it, it is necessary to combine the forces of aviation authorities, industrial enterprises, science, and civil aviation organizations. Their consolidated efforts should be aimed at reducing safety risk in both civil and general aviation taking into account the new ICAO standards and recommendations (Amendment No. 172 (2014) to Annex 1 “Personnel Licensing” to the Chicago Convention; Chapter 3 of PANS-TRG “Training” (Doc 9868, Second Edition, 2016); Doc 10011 “Manual on Aeroplane Upset Prevention and Recovery Training” (First Edition, 2014)).

Airplane stall is an uncontrolled flight mode which occurs due to loss of stability and control at high angles of attack, in which airplane movements do not correspond with control movements and change abruptly and unpredictably.

Airplane Upset State (UAS) is an undesired airplane state characterized by unintentional divergences from parameters normally experienced during operations. Both of the terms (‘Stall’ and ‘Upset’) have many common features [6].

Loss of Control In-Flight means not only deterioration in stability and performance and/or a complete loss of control, but also a shortage or lack of knowledge on how to handle a situation that has arisen unexpectedly and is very different from the standard operational flight mode.

Article [7] discusses in detail the physical aspects of loss of control as a result of stall at high angles of attack and algorithms for stall mode diagnostics and airplane protection from inadvertently encountering post stall gyration and entering spin modes. It summarizes the results of the linear theory of stall developing as the theoretical foundation for a nonlinear approach to detecting flight conditions related to loss of aircraft control which is understood as the moment when the angular rates exceed some critical (threshold) values, which in general depend on the angle of attack and airspeed and they correspond to control surfaces deflection.

Along with stalling, another serious threat to flight safety lies in atmospheric disturbances, which can make significant and unexpected changes to the values of the most important flight parameters, such as angles of attack and slip ( $\Delta\alpha, \Delta\beta$ ) and flying speed  $\Delta V$ , whose dominant influence on the flight dynamics of an aircraft is obvious since they determine the magnitudes of aerodynamic forces and couples acting on the aircraft.

Atmospheric disturbances (see Fig. 2) can be caused by natural atmospheric phenomena, including vertical and horizontal gusts (wind shear), mountain waves and vortex rings, as well as aircraft and helicopter trailing vortices.

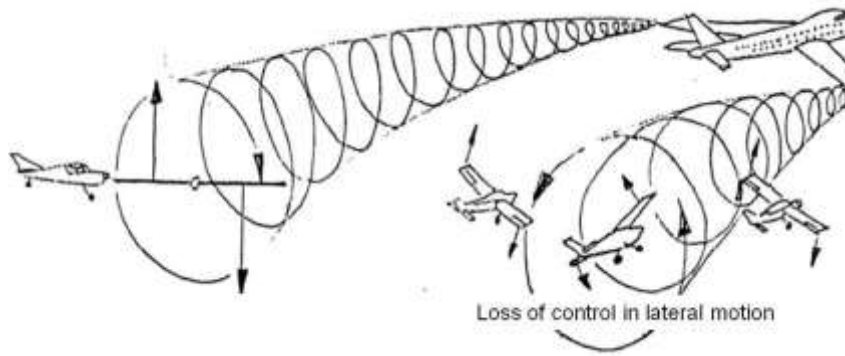


Fig. (3).A light aircraft hitting a trailing vortex from a heavy aircraft flying.

Table 1. Wind Shear Intensity Criteria.

Wind shear Intensity (Qualitative Parameter)	Vertical Wind Shear (Updraft and Downdraft) Per 30 m; Horizontal Wind Shear Per 600 m, m/s	Influence on Aircraft Control
Weak	0-2	Insignificant
Moderate	2-4	Significant
Strong	4-6	Dangerous
Very strong	more than 6	Very dangerous

As a rule, wind shear occurs near or under cumulonimbus clouds, in atmospheric front zones, in the presence of inversion near the ground, as well as in mountainous and coastal areas. Sharp changes in wind conditions are especially dangerous if they happen near the ground along the trajectory of the aircraft, as they may occur unexpectedly for the crew. The aircraft moves through the planetary boundary layer so quickly that small altitude and speed margins and a limited time for engine acceleration do not always allow the crew to react timely to sharp changes in wind direction, which is one of the main causes of flight accidents. In order to tackle this issue, ICAO and the Commission for Aeronautical Meteorology at WMO have issued joint resolutions where it is stated that it is necessary to provide crews with detailed information on wind changes in the lowest layer of the atmosphere when taking off and landing.

Wind shear presents an even bigger danger to light and ultra light aircraft as they have low weight, relatively low flying speed, and low thrust-to-weight ratio.

Hitting a vortex from another aircraft is an issue encountered most often near aerodromes due to the high intensity of air traffic and short distances in space (in terms of both lateral and vertical separation). This issue is of importance to civil aviation both as a safety issue and a factor which influences airspace capacity.

Accidents usually occur when a light aircraft hits a trailing vortex from a heavy aircraft flying ahead of it. As shown in Fig. 3, an aircraft flying through a turbulent wake can be subjected to heavy and sudden vertical loads and a plane flying along a turbulent wake can start rotating uncontrollably [8].

If a small aircraft hits a trailing vortex from a large aircraft, it may even cause structural failures in the smaller aircraft.

### 1. WIND DISTURBANCES CAUSED BY WIND SHEAR

Atmospheric turbulence is a state characterized by irregular air motions that vary in speed and direction. The main cause of turbulence is differences in temperature and wind direction.

When flying through vortices, the aircraft is exposed to vertical and horizontal loads, which take the form of gusts of wind. As a result, the equilibrium of aerodynamic forces acting on the aircraft becomes disrupted, and the aircraft starts flying out-of-balance. If flight disturbances accumulate, it can lead to a potentially dangerous loss of altitude and, subsequently, a collision with the ground.

A sudden change in wind speed and/or direction can happen both in the horizontal direction (horizontal wind shear) and the vertical direction (vertical wind shear). Vertical wind shear is a change in wind speed and/or direction with change in altitude. A vertical wind shear of 4-6 m/s or more (including both updraft and downdraft) per 30 m is considered to be dangerous if it occurs near the aerodrome. Take-off or landing permission in such a situation is denied.

Vertical wind shear has nonlinear dependence on the thickness of the air layer. Within the same layer, updraft and downdraft may differ in their force.

Wind shears are classified not only by direction (vertical or horizontal), but also by intensity (Table 1).

At present, there are no sufficiently reliable methods of either detecting or predicting wind shears along descending or take-off flight paths. Airport personnel use data from constant-level balloons, wind-detecting gadgets installed on tall buildings located near the aerodrome or on television masts, or from special equipment (Doppler radars etc.). If this data is not

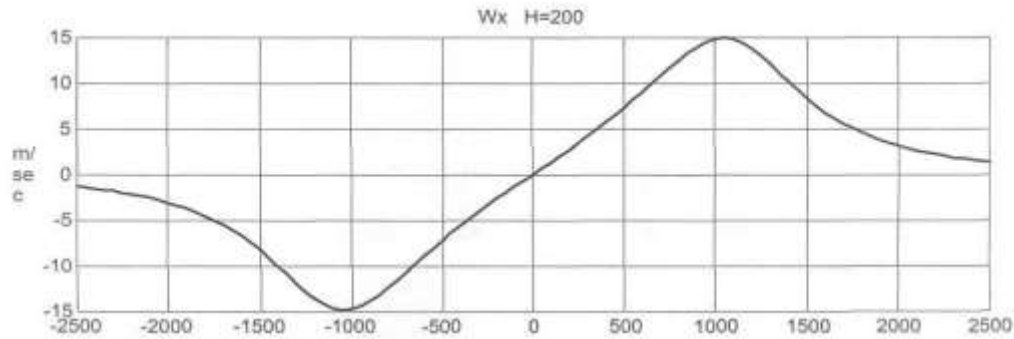


Fig. (4).The horizontal component Wx of the wind profile at H = 200 m.

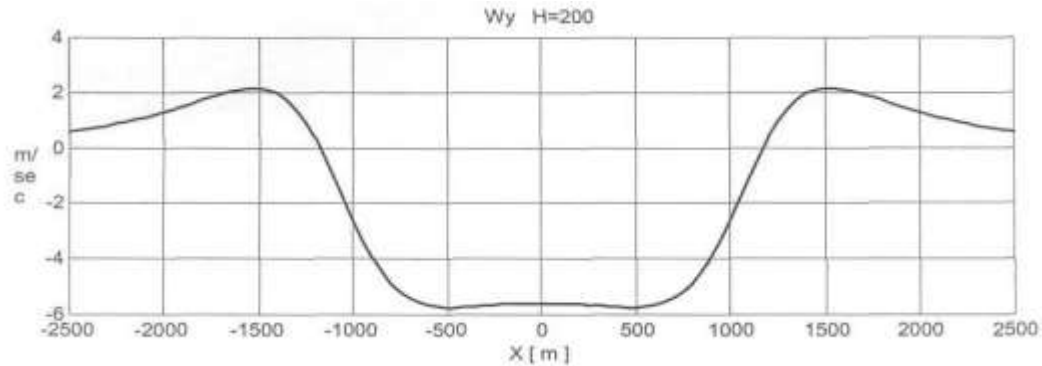


Fig. (5).The vertical component Wy of the wind profile at H = 200 m.

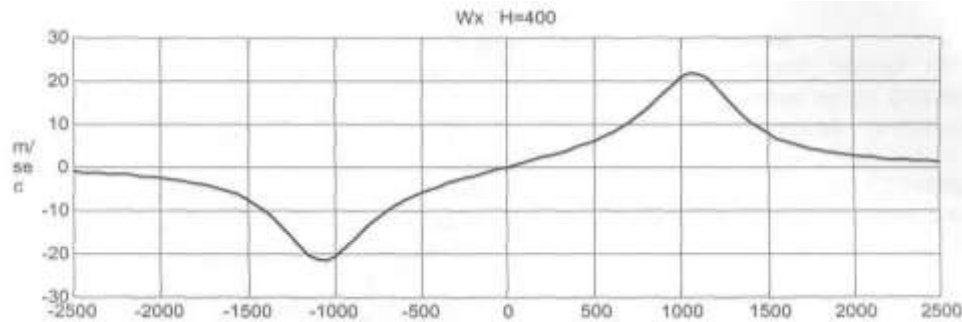


Fig. (6).The horizontal component Wx of the wind profile at H = 400 m.

available, it is necessary to use wind forecast charts. The possibility of detecting wind shears using laser technology is being studied.

During pre-flight preparation and the final approach, flight crew must bear in mind that some weather conditions favour the occurrence of strong wind shears during takeoff and landing, and that wind shears are invisible, dangerous, and occur unexpectedly.

**2. WIND SHEAR SIMULATION (DOWNBURST)**

This paper focuses on downbursts, which present the greatest danger to aircraft flying at low altitudes as well as taking off and landing.

Source [9] contains data on the parameters of downbursts based on wind profile measurements in the situations which led to the crash of the Boeing-727 aircraft taking off in New Orleans in 1982 and the crash of the L-1011 landing in Dallas in 1985.

Fig. (4-7) show the graphs of the vertical (Wy) and horizontal (Wx) components of the wind profile in the microburst zone at two different heights (H = 200m and H = 400m).

This wind disturbance can be described using the mathematical model proposed by M. Ivan in [10], in which the microburst area is formed by a flow around a toroidal vortex ring which is located above a flat surface. In this model, all characteristics of the flow can be expressed as a current function of a three-dimensional vortex-free movement of an incompressible flow induced by a vortex ring, which can be described using the following equation:

$$\Psi = -\frac{\Gamma}{2\pi} (r_1 + r_2)(K(\lambda) - E(\lambda)),$$

where  $\Gamma$  is circulation,  $r_1$  and  $r_2$  are the smallest and greatest distances from the current point  $(x, z, h)$  to the vortex line,  $\lambda = (r_2 - r_1)/(r_2 + r_1)$ ,  $K(\lambda)$  and  $E(\lambda)$  are complete elliptic integrals of the first and second kinds. Geometric relationships are shown in Fig. (8).

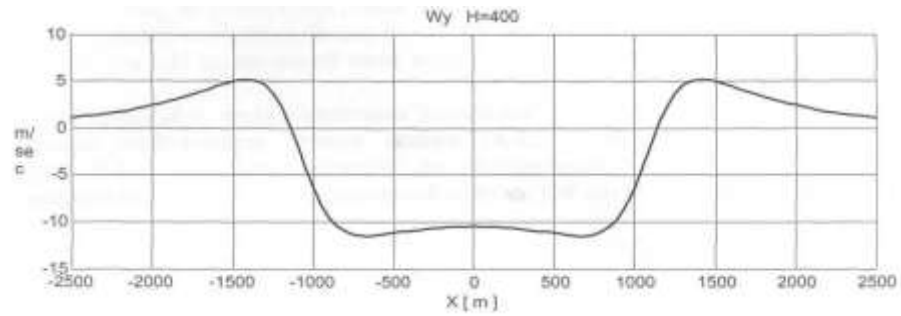


Fig. (7).The vertical component Wy of the wind profile at H = 400 m.

Table 2. Model parameters.

Parameter	Unit of Measurement	Model 1	Model 2
G	m2/s	23755	41319
Rc	m	152.5	122
H	m	889	689
R	m	1019	1090

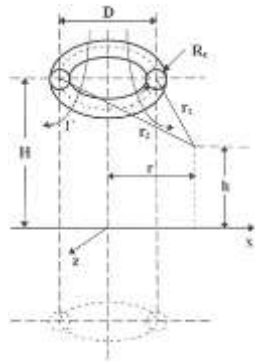


Fig. (8).A toroidal vortex ring above a flat surface.

R is the radius of the vortex line, Rc is the effective kernel radius of the vortex ring. The velocity field induced by the vortex line is determined by five parameters: the position of the centre of the ring (x, z, h), circulation ( $\Gamma$ ), and the radius (R). The x, z, and h parameters affect the relative position, but not the way velocities are distributed. G produces a linear effect and R is a scale factor. The parameters of the model suggested by M. Ivan are given in Table 2.

In order to simplify the calculation process, M. Ivan suggests in his paper [10] that equations with elliptical integrals should be approximated as follows:

$$K(\lambda) - E(\lambda) = \frac{\pi \lambda^2}{1+3\sqrt{1-\lambda^2}}, \text{ where } 0 \leq \lambda \leq 1$$

Having simplified the equation of the current function, we will express the components of the wind speed in three-dimensional space (x, y, z) in the microburst zone as follows:

$$W_x = -\frac{x}{r^2} \frac{d\Psi}{dy}$$

$$W_z = -\frac{z}{r^2} \frac{d\Psi}{dy}$$

$$W_y = \frac{1}{r} \frac{d\Psi}{dr}, \text{ where } r = \sqrt{x^2 + z^2}$$

Let us compare the model of wind disturbances with the experimental data obtained by Zhao Y [9].

The results of comparing the model and the experimental data are shown below in Fig. (9-10).

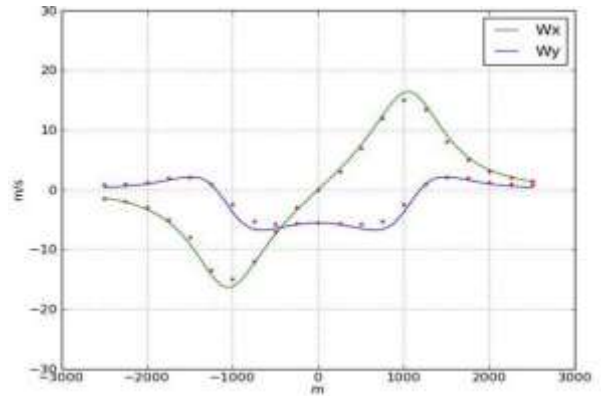


Fig. (9).Wind speed profiles for H = 200m

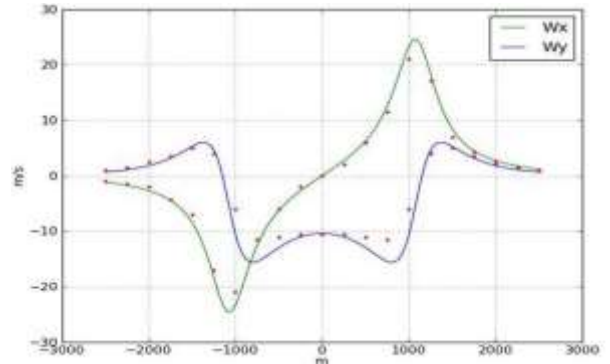


Fig. (10).Wind speed profiles for H = 400m

The solid lines in the graphs show the velocities calculated using the vortex ring model proposed by M. Ivan. The dotted lines show the velocities according to the experimental model by Zhao Y.

The comparison shows that the vortex ring model proposed by M. Ivan describes wind disturbances arising from wind shear quite well.

### 3. ATMOSPHERIC DISTURBANCES IN MOUNTAIN ROTORS

Paper [11] contains very interesting calculations of flow lines in the wind velocity field of an air mass located in a mountainous area which is blown by a fairly strong wind with a constant direction. Fig. (11) presents a visualization of vortices using a three-dimensional texture and the ray tracing method. The visualization was made by the authors of the paper.

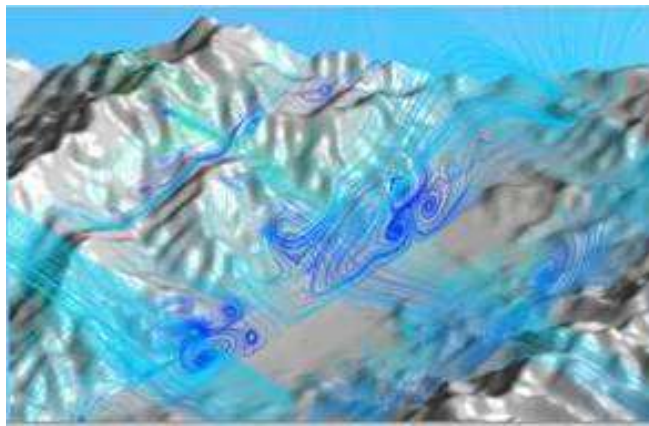


Fig. (11). The visualization of the flow field in a mountainous area.

The results of the experiments conducted by American scientists in the Sierra Nevada, California, in 2004 using gliders, atmospheric monitoring stations, and constant-level balloons [12-14] can serve as a proof of the calculations presented in paper [11]. The model of mountain waves which was developed after conducting a series of experiments looks as follows (see Fig. 12):

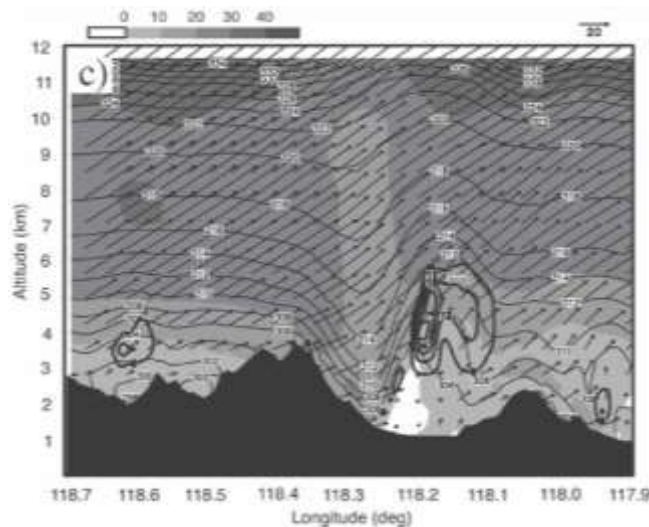


Fig. (12). The experimental model of mountain waves with rotors.

It can be seen that rotors in the experimental model appear in depressions between two obstacles (mountain folds), which means that it is possible to use the mathematical model proposed in [11] in flight simulator tests to study flight conditions over mountainous areas with similar topographic features. This research could be continued by analyzing the dependence of rotor sizes and temperature profiles in mountainous areas on the shape of topographic features and the exact conditions for the formation of rotors in the mountains.

Fig. (13) shows vertical and horizontal wind disturbance profiles in the rotor area (the centre of coordinates (OxH) coincides with the vortex core). The vertical component ( $\Delta W_y(x)$ ) does not change in its profile depending on H, but the parameter  $\Delta W_y(x)$  will decrease from  $W_y \max$  to zero during movements from HV to H2 and from HV to H1.

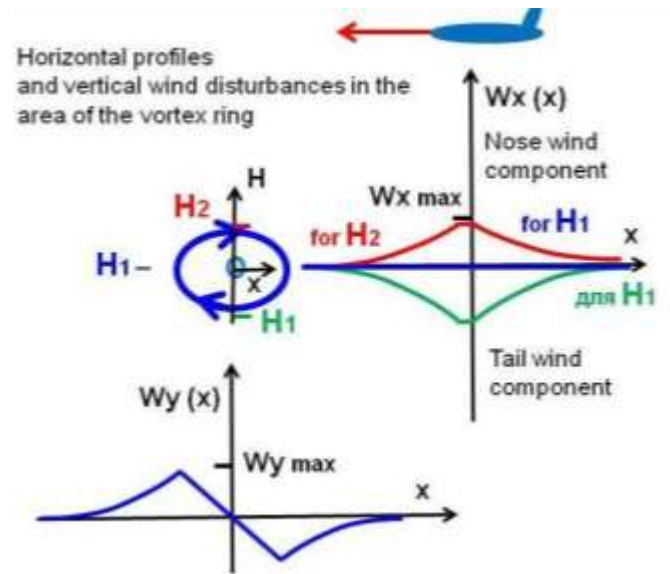


Fig. (13). Wind disturbance profiles in the rotor area.

Fig. (14) shows the flow field as well as vertical and horizontal wind disturbance profiles in the wave area above mountain folds (the centre of coordinates (OxH) coincides with the centre of the wave). The equidistance of the flow in terms of height results in the fact that  $\Delta W_x(x)$  и  $\Delta W_y(x)$  do not change depending on H and will be the same at HB, H2 and H1.

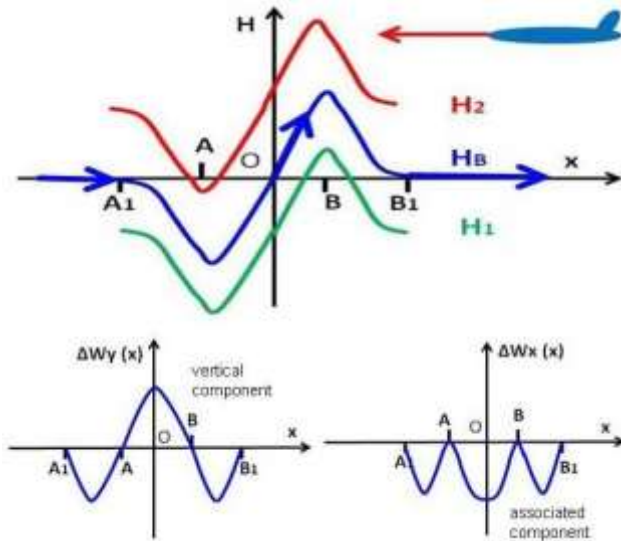


Fig. (14). Wind disturbance profiles in the wave area.

#### 4. ATMOSPHERIC DISTURBANCES CAUSED BY TRAILING VORTICES

The characteristics of a trailing vortex depend on the type of aircraft and its in-flight weight. The flow pattern in a trailing vortex is well-illustrated by the drawing and photographs shown in Fig. (15).



Fig. (15). The flow pattern in a trailing vortex.

The diameter of wingtip vortices can amount to 8-15 meters, and their peripheral speed can reach 150 km/h. Hitting a trailing vortex can cause an increase in roll rate (up to 200 degrees per second), loss of altitude (up to 150-200 meters) and, ultimately, loss of control. This is especially dangerous during the final approach if there is not enough vertical clearance.

Let us consider an example of the impact of a trailing vortex on an airplane. If the plane enters zone I of the trailing vortex (Fig. 16) or approaches it from the right, it experiences a roll moment disturbance directed to the right. As a result, the aircraft is subjected to significant overload from the wingtip vortex area with an angular velocity of up to 200 °/s. Loss of altitude can amount to 150 ... 200m. If the plane enters zone II, it will result in a left roll to 130°. Entering zone III will result in a right roll. In the latter case, the plane may experience such strong pressure from the disturbances in the trailing vortex that the flight control surfaces might fail to counteract this pressure.

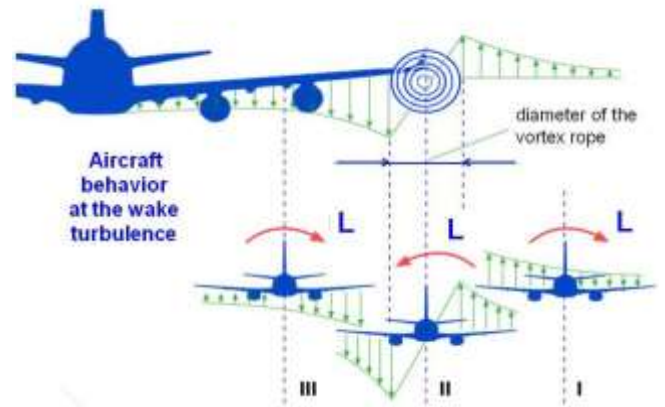


Fig. (16). An example of the impact of a trailing vortex on an airplane.

When the airplane enters wake turbulence, it becomes subjected to additional aerodynamic forces, which may result in airplane upset. An important task for specialists is to develop criteria for assessing whether the impact and consequences of turbulence should or should not be considered acceptable from the safety point of view. ICAO has developed such criteria for long-haul aircraft and they are used in practice. According to these criteria, airplane upset is defined by the existence of at least one of the following parameters:

- a) pitch attitude greater than 25 degrees, nose up; or
- b) pitch attitude greater than 10 degrees, nose down; or
- c) bank angle greater than 45 degrees; or
- d) within the above parameters, but flying at airspeeds inappropriate for the conditions

#### 5. ATMOSPHERIC DISTURBANCES CAUSED BY A HELICOPTER

The flow pattern in a trailing vortex from a helicopter is shown in Fig. (17-19).

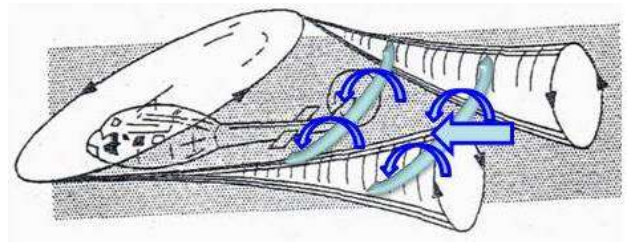


Fig. (17). A drawing of the flow pattern in a trailing vortex from a helicopter

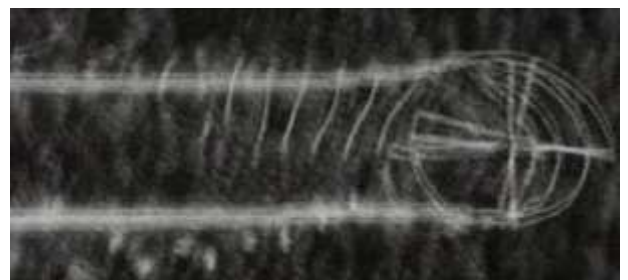


Fig. (18). The flow pattern in a trailing vortex from a helicopter (top view)



Fig. (19). The flow pattern in a trailing vortex from a helicopter (side view)

As can be seen in the pictures (Fig. 17-19), there are wake vortices (the so-called ‘stairs’) apart from wingtip vortices. In addition to other things, the wake from a low-flying helicopter causes a nose-down pitching moment and a tail wind flow, as shown in Fig. (20), due to the fact that the wake vortices gather and roll one after another along the terrain.

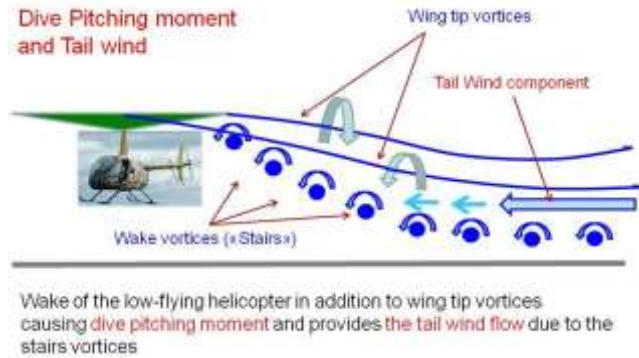


Fig. (20). The flow pattern in the wake from a low-flying helicopter.

A hovering helicopter also causes disturbances in the atmosphere, which can also be dangerous, especially if the helicopter is hovering low above the ground. The flow pattern from a hovering helicopter is shown in Fig. (21).

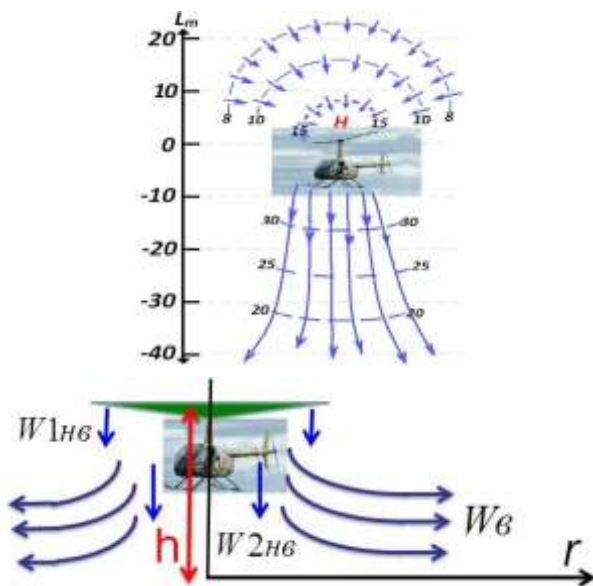


Fig. (21). The flow pattern from a hovering helicopter.

It is possible to calculate the speed of the wind flow ( $w_B$ ) diverging in all directions from a helicopter hovering low

above the ground using the law of momentum conservation and the Joukowski theorem about doubling inductive speed on hover [15].

$\mu$  is air flow through the helicopter main rotor:

$\mu = w_{1HB} \cdot \rho \cdot S_{HB}$ , where  $S_{HB}$  is the rotor disk area,  $w_{1HB}$  is the induced velocity of the flow coming from the rotor, and  $\rho$  is air density.

Then, where  $m$  is the mass of the helicopter.

As follows from the Kutta–Joukowski theorem, the hover-induced velocity is doubled ( $w_{2HB} = 2 w_{1HB}$ ), and, consequently,

$$W_{2HB} = 2\sqrt{mg / 2\rho S_{HB}}$$

As follows from the balance between the force of gravity and the rotor lift ( $T_{HB}$ ) ( $w_{2HB} \cdot \mu = T_{HB} = mg$ ) and the law of conservation of mass,

$$\rho \cdot 2\pi \cdot r \cdot h \cdot w_B = \rho \cdot w_{HB} \cdot S_{HB},$$

where  $h$  is the hovering height, and  $r$  is the horizontal distance from the helicopter.

Hence the equation

$$W_B(r) \approx \sqrt{2mgS_{HB} / \rho} \cdot \frac{1}{2\pi \cdot r \cdot h}$$

This equation can be used for determining the speed of the helicopter-induced airflow at the  $r$  horizontal distance from the helicopter having an  $m$  mass, an  $S_{HB}$  rotor disk area and hovering at an  $h$  height (see Fig. 22). For example, the R-66 Robinson helicopter having a mass of 1,200 kg, the main rotor diameter  $D_{HB} = 10$  m, and accordingly, the  $S_{HB}$  area = 75 sq m will induce an airflow with a velocity of 5 m/s at a distance of 15 m from itself when hovering at a height of 3 m ( $w_B = f(r, h)$ ). At the same time, the Ka-32 helicopter having a mass of 12,000 kg, the main rotor diameter  $D_{HB} = 16$  m, and the  $S_{HB}$  area = 200 sq m will induce an airflow with a velocity of 15 m/s at a distance of 20 m from itself when hovering at a height of 5 m.

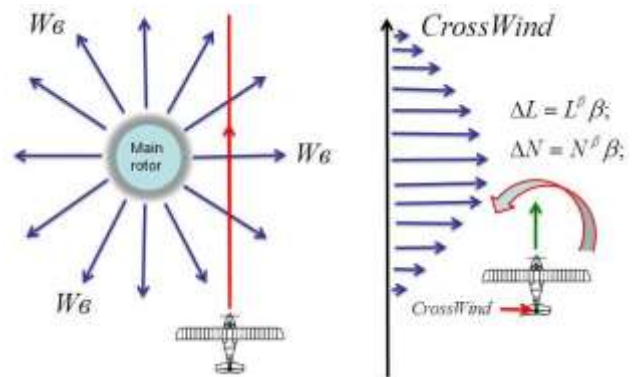


Fig. (22). Air flows from a helicopter hovering above the ground.

Diverging air flows create crosswinds influencing an aircraft passing by.

One day, when one of the authors of this paper was performing a takeoff on a light airplane (MTOW = 530 kg), he

all of a sudden hit the wake of a heavier helicopter (MTOW = 1200 kg), to which the air traffic controller, who had already allowed the plane to take off, allowed a parallel passage at the windward side of the runway (Fig. 23).

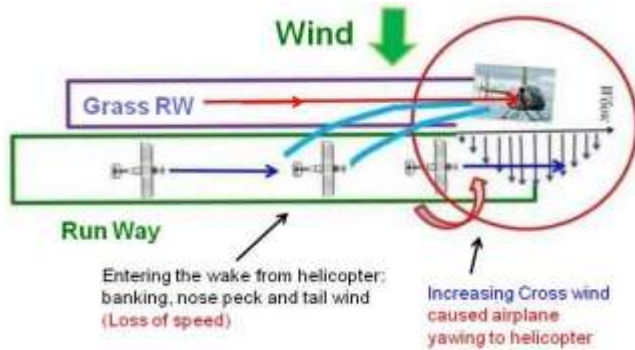


Fig. (23). An airplane hitting the wake of a helicopter while taking off.

The right rotor wing tip vortex from the helicopter caused a bank disturbance of the airplane to the left (left roll rate) and the wake vortices provided a tail wind flow followed by a loss of airspeed and simultaneously caused a dive pitching moment followed by a nose-down. At that moment, the airplane was at an altitude of three to four meters from the ground. The pilot, carefully watching the airspeed value and eliminating the bank angle, understood that the only way to handle this situation was to push the control stick forward proportionally in order to reduce the angle of attack, to decrease the inductive drag force  $D = qS C_D = qS (C_{D0} + kC_L^2(\alpha))$  due to decreasing angle of attack, and to increase the airspeed due to gravity force component  $mg \sin \gamma$  as it is shown at Fig. (24) ( $q$  – dynamic pressure,  $\gamma$  – flight path angle).

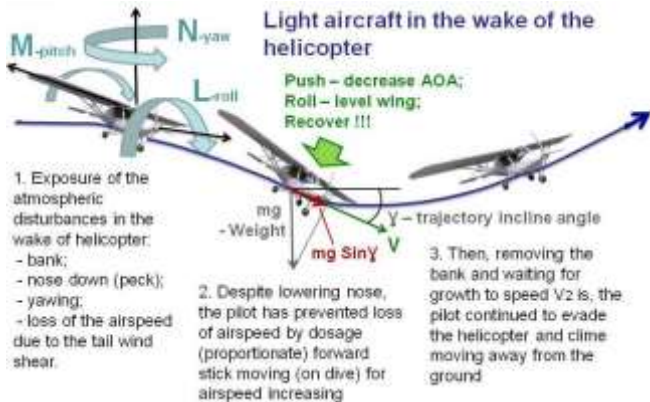


Fig. (24). An airplane hitting the wake of a helicopter while taking off.

The pilot felt an urge to pull the control stick back in order to lift up the nose of the airplane, but his knowledge and experience suppressed that urge. If it had not happened, the aircraft would have stalled, which, unfortunately, has happened a number of times in similar situations all around the world.

It was not the end though. The air traffic controller, who did not notice what had happened, allowed the helicopter to hover over the runway. As a result, after exiting the helicopter wake turbulence area, the airplane got into another flow area as is shown in Fig. (22 and 23) (the red circle). To overcome the increasing slip, the pilot had to completely deflect the pedals.

It seemed that this nightmare had lasted for 20-30 seconds. Thanks to a video camera installed aboard, it was possible to watch and analyze the video recording of the accident. As the video showed, the whole breathtaking accident lasted for only five seconds. This is how adrenaline slows time down in emergencies.

## 6. METHODS OF PROTECTION AGAINST ATMOSPHERIC DISTURBANCES

Let us consider a few possible ways and methods of protecting aircraft from dangerous atmospheric disturbances arising from wind gusts and wakes from aircraft (both airplanes and helicopters).

### 6.1. Methods of protection against hitting a wake

Detailed information on the characteristics of trailing vortices and their effect on aircraft is given in the Air Traffic Services Planning Manual (Doc 9426, Part II, Section 5, Chapter 3, Paragraph 3.2.1.2).

Detailed information on separation minima is also given in the Air Traffic Services Planning Manual (Doc 9426, Part II, Section 5, Chapter 3, Paragraph 3.2.4).

There are a few acceptable intervals between aircraft moving in the air (see Fig. 25).



Fig. (25). Acceptable intervals between aircraft moving in the air.

It is possible to calculate these intervals automatically by using on-board and ground vortex information systems which should use data exchange interfaces sharing data on the mass, coordinates, and speed of aircraft located in a specific segment of airspace and posing a threat to each other. Some work in this direction is currently being done.

### 6.2. Automatic Protection Against the Consequences of Hitting a Microburst

#### 6.2.1. Microburst Detection Algorithm

Automatic control could be one of the methods of protecting aircraft from dangerous atmospheric disturbances. On-board equipment has always played a huge role in the aircraft industry. As its quality gradually improved, it became easier and safer to fly aircraft and it took less time to train flight crew. Currently, remote control system and on-board computers handle the majority of flying operations themselves. Developing an on-board wind shear detection system would follow the current trend towards automation and definitely find its application in real life.

This paper describes an algorithm that was developed for:

- detecting the situation of hitting a wind shear zone;
- informing the crew about the danger;

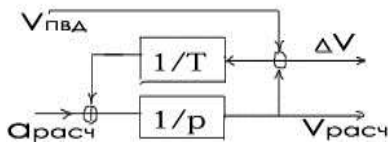
- allowing the airplane to exit the wind shear zone in the shortest time possible.

We tested the algorithms using the Sigma-Classic simulator having FNPT Level II according to the JAR-FSTD-A standards. This simulator is installed at School № 14 in the town of Zhukovsky, Moscow Region, Russian Federation.

Due to the fact that ultra light aircraft can take off from fields, unpaved roads, or abandoned aerodromes, where there are no weather services and no information about wind shears either, and the fact that not all light aircraft are equipped with meteorological devices capable of detecting wind shears, a question arises: how is it possible to detect whether the airplane has hit a wind shear if it has only an air data system, an attitude and heading reference system, and accelerometers at its disposal?

The main idea shared in this paper is that when an airplane hits a gust of wind, the indicated air speed will increase due to headwind, while the airplane will be slowed down by the headwind. This means that it is necessary to monitor if there is a difference between the indicated airspeed and the estimated airspeed, which is determined by integrating the readings from the accelerometers. The estimated airspeed can be determined using the signals from the accelerometers and the attitude and heading reference system.

However, due to the approximation error there will be an error in the estimated speed. Therefore, we will correct the estimated speed as follows:



This diagram can be presented as a set of equations:

$$\frac{d V_{\text{расч}}}{d t} = \ddot{a} + \frac{\Delta \dot{V}}{T}$$

$$\Delta \dot{V} = V_{\text{ПВД}} - V_{\text{расч}}$$

$V_{\text{расч}}$  is the estimated speed,  $V_{\text{ПВД}} = V_i$  is the airspeed calculated using the data from pitot tubes,  $\ddot{a}$  is the acceleration vector in the wind axis coordinate system,  $T$  is the characteristic time for correcting the estimated speed (it is determined by the characteristics of the accelerometers and the sensitivity of the pitot tubes).

Thus, if we monitor the  $\Delta V$  difference and see that the value determined by the sensitivity of the pitot tubes is exceeded, we can say that the plane has hit a wind shear and inform the pilot about it.

**6.2.2. A Search for Optimal Parameters Allowing the Aircraft to Exit the Wind Shear Zone**

Such a parameter as vertical clearance is among the key ones when an aircraft is flying through a downburst area. After we discover that the airplane has hit a wind shear zone, a question arises: what should the pilot do in order to recover with a minimal loss of altitude?

Let us analyze this situation using the example of the Sigma-Classic aircraft. The dependences of climb rate  $V_y$  on  $V_i$  (for this aircraft are presented in Fig. 26).

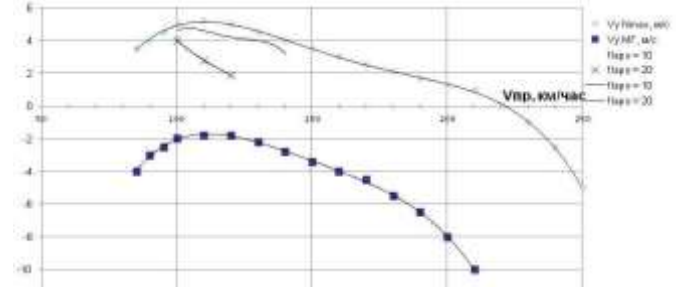


Fig. (26).Polar curves of the Sigma-Classic aircraft.

Climb (or dive) rate  $V_y$  and  $V_i$  are vertical and indicated airspeeds at different positions of the flaps:  $0^\circ$  of flaps,  $10^\circ$  of flaps,  $20^\circ$  of flaps. We will make an assumption that compressibility factors are insignificant at relatively low flying speeds and low altitudes and the difference in air density between the altitude level and the ground level is negligible.

Given this assumption,  $V_{pr} \approx V$ , where  $V$  is the true airspeed.

In the earth’s coordinate system, the velocity components will look as follows:

$$V_{x_g} = V_x + W_x$$

$$V_{y_g} = V_y + W_y$$

where  $V_y$  is the vertical speed of the aircraft relative to the air mass, which can be presented in the following way based on the polar curve:

$$V_y = f(V)$$

$V_x$  is the horizontal speed of the aircraft relative to the air mass,

$$V_x = \sqrt{V^2 - V_y^2} = \sqrt{V^2 - f(V)^2}$$

Let us assume that it will take an aircraft a period of  $dt$  to fly over a distance  $dr$  with a speed of  $V_{xg}$  in a microburst.

$$dt = \frac{dr}{V_{xg}}$$

Then a change in height ( $dH$ ) over a period of time ( $dt$ ) will be:

$$dH = V_{y_g} * dt$$

By substituting the previous equations into this expression, we will get:

$$dH = (V_y + W_y) * \frac{dr}{V_{xg}} = \frac{(f(V) + W_y(r))}{\sqrt{V^2 - f(V)^2 + W_x(r)}} * dr$$

As a result of integrating, we will have:

$$H = \int_{-L}^L \frac{(f(V) + W_y(r))}{\sqrt{V^2 - f(V)^2 + W_x(r)}} dr$$

, where  $L$  is the characteristic microburst size.

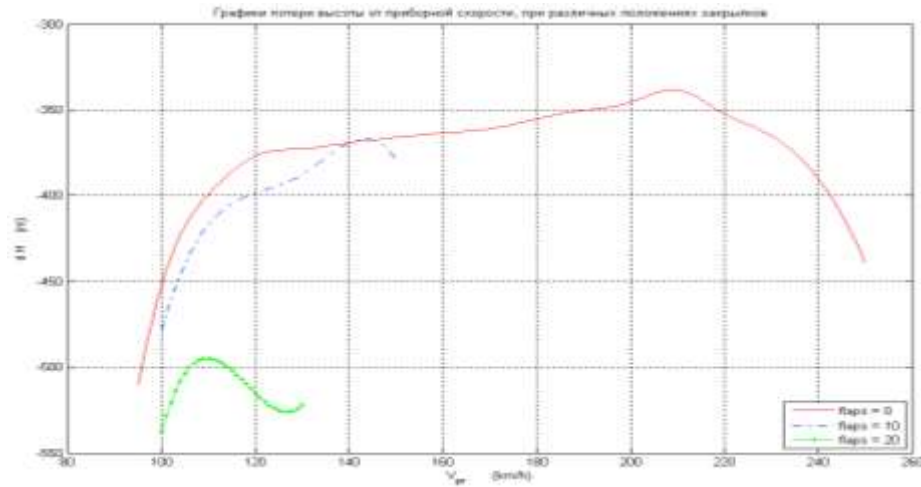


Fig. (27). Loss of altitude depending on the indicated airspeed.

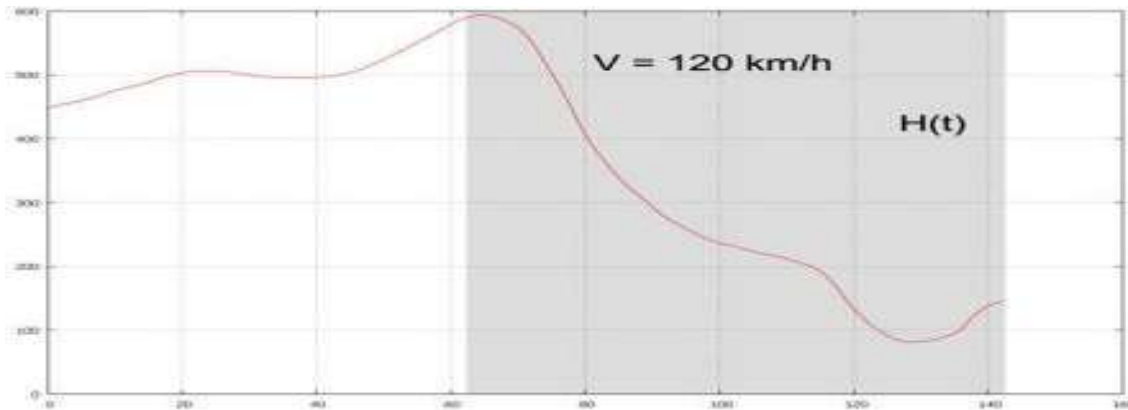


Fig. (28). Simulation results at V = 120 km/h.

As the  $W_y(r)$  function is even and the  $W_x(r)$  function is odd, we will simplify the equation:

$$W_y(-r) = W_y(r)$$

$$W_x(-r) = -W_x(r)$$

Then

$$H = 2\sqrt{V^2 - f(V)^2} \int_0^{L/2} \frac{(f(V) + W_y(r))}{V^2 - f(V)^2 - W_x(r)^2} dr$$

Let us build graphs using the equation. The dependence of loss of altitude on the indicated airspeed is shown in Fig. (27). The red line represents 0° of flaps, the blue line represents 10° of flaps, and the green line represents 20° of flaps.

We got an interesting result which is contrary to the feeling that loss of altitude will be the smallest if the plane flies at the maximum  $V_y$  vertical speed or the maximum limit speed.

The graphs clearly show that there is a peak point for each flight mode. For example, when flying with 0° of flaps, loss of attitude will be the smallest if the aircraft flies at about 210 km/h while the maximum limit speed for this type of aircraft is 250 km/h. This means that after the system detects that the aircraft has hit a wind shear zone, the pilot or the autopilot system (if there is one) should maintain an indicated air speed

of 210 km/h with 0° of flaps in order to ensure a minimum loss of attitude.

### 6.2.2. Simulation Results

We used all the results presented above (the mathematical model of a downburst, the algorithm for detecting the situation of hitting a wind shear zone) in further Sigma-Classic simulator tests. We designed an algorithm for exiting a wind shear zone based on the conclusion made in the previous paragraph, according to which the pilot should maintain a particular speed with 0° of flaps in order to ensure a minimum loss of attitude in the microburst area.

Fig. (28-30) show the results of modelling flights through a wind shear zone at different speeds (120 km/h, 150 km/h, 210 km/h). Different speeds were analyzed in order to see changes in loss of attitude.

The graphs show the dependence of height (H), indicated airspeed ( $V_i$ ), vertical speed ( $V_y$ ), and the difference between indicated and estimated speeds ( $\Delta V$ ) on time. The grey areas indicate the periods of time when the aircraft was flying through a downburst area.

As can be seen, the smallest loss of attitude happens at a speed of 210 km/h, which is in accord with theoretical calculations. Significant differences between the airspeed and the estimated

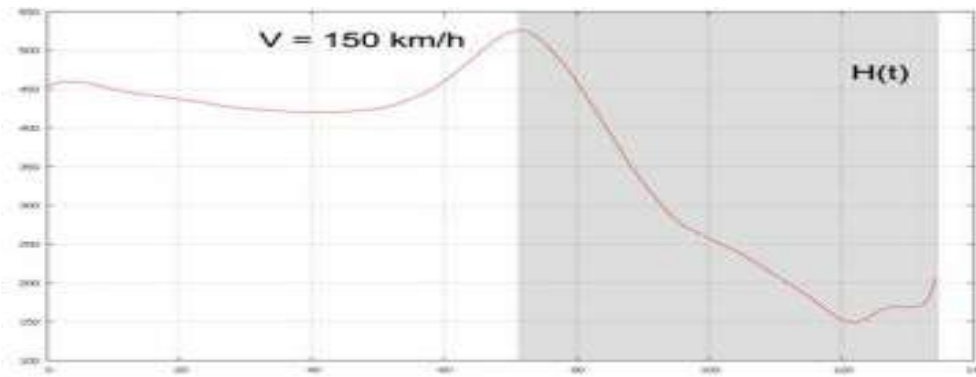


Fig. (29).Simulation results at V = 150 km/h.

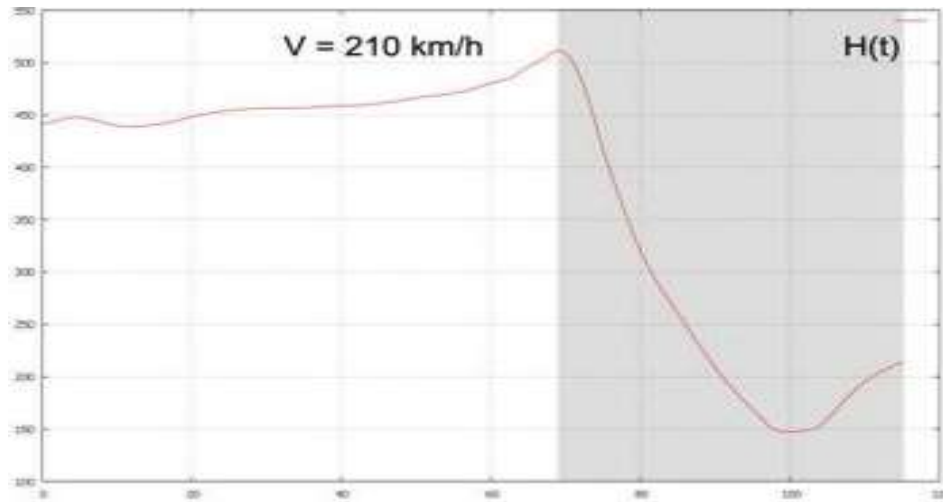


Fig. (30). Simulation results at V = 210 km/h.

Table 3. Upset Prevention, Recognition & Recovery Training (UPRT).

Upset	- We do not understand what’s going on with the aircraft ... "- What kind of failure is it...?" / ATR-42 Cpt. - Tyumen, 2012/
Prevention,	- We do not know how to prevent the development of this situation ...
Recognition	- We have never seen this ... We have never encountered it before ...
& Recovery	- We do not know how to get to the operational flight envelope ...
Training	- We need to learn about such things in advance!

speed start manifesting themselves outside the radius of the vortex ring, which means that if the crew members get a timely notification, they will know that they are about to enter a vortex and microburst area. Thus, the results of this semi-natural experiment confirm the results of calculations, which means that the proposed algorithm can be used to protect aircraft from entering microburst areas.

**CONCLUSION**

1. An algorithm for detecting wind shear which can be implemented in on-board systems for detecting critical situations has been proposed.
2. The best way of recovering with a minimum loss of attitude after entering a wind shear zone has been found. A method for selecting the optimal speed for a particular aircraft based on its aerodynamic polar curves has been developed.

3. Algorithm efficiency has been tested in a semi-natural experiment using a simulator. The results have proven that the algorithm is efficient.

**POSTSCRIPT**

Along with the development of on-board systems for detecting critical conditions, it is necessary to improve the qualification performance standards for flight simulator training devices (FSTD) in order to extend the range of flight conditions and provide an opportunity for training under adverse weather conditions. It will enable pilots to learn how to assess critical situations correctly and recognize the real reason for loss of control in flight, and it will also help them to master their upset and stall prevention and recovery skills. This is one of the main aspects of upset prevention and recovery training according to Doc. 10011 by the ICAO (see table 3).

It is very important to develop theoretical and simulator training programs for pilots in order to improve their skills in upset prevention, recognition and recovery so that they could use them in case of loss of control.

### CONFLICT OF INTEREST

The authors declare no conflicts of interest.

### REFERENCES

- [1]. J. Nall, General Aviation Accidents in 2011, 23-th Report. Maryland: Air Safety Institute, a division of AOPA foundation, 2012. – 48 p., General aviation safety. Additional FAA Efforts Could Help Identify and Mitigate Safety Risks. Washington: GAO 2012; 44.
- [2]. State of Global Aviation Safety. Montreal: International Civil Aviation Organization 2013; 54 .
- [3]. State of Civil Aviation Safety in Member States of the Agreement on Civil Aviation and Use of Airspace in 2014. Moscow: Interstate Aviation Committee 2015; 72.
- [4]. State of Global Aviation Safety. Special Edition. Montreal: International Civil Aviation Organization 2011;80.
- [5]. Reports of investigated air accidents in civil aviation in 2005-2014. Materials of the Interstate Aviation Committee (IAC).
- [6]. Eric Denoux. UPRT – Airbus Flight Operations & Training symposium, Moscow Fhril 2018; 24-25.
- [7]. Critical Flight Conditions at High Angles of Attack, Related to Loss of Control in Lateral Motion. Advances in Military Technology 2016; 11(1).
- [8]. Afanasyeva LA, Khlopkov YuI, Chernyshev SL. Aerodynamic Aspects of Flight Safety. Introductory Course. Moscow: Moscow Institute of Physics and Technology 2011 ;184pp .
- [9]. Zhao Y. A Simplified Ring-Vortex Downburst Model. // AIAA Paper. No. 580, 1990, pp. 1-11
- [10]. M. Ivan. A Ring-Vortex Downburst Model for Flight Simulations. J. Aircraft 1986;23: 3.
- [11]. V.V. Vyshinsky, V.K. Ivanov, A.V. Terpugov. Simulations of Difficult Flight Conditions in the Context of Atmospheric Turbulence. Proceedings of MIPT 2015;7(1).
- [12]. Hodur, R.M., The Naval Research Laboratory's Coupled Ocean / Atmosphere Mesoscale Prediction System (COAMPS). Mon. Wea. Rev 1997; 125: 1414-30.
- [13]. B. Billings.IOP 8. The Atrac Leopens rotor event of Sierra Rotors. J. Atmos. Sci 2007; 64: 4178–4201
- [14]. Scorer RS. Theory of waves in the lee of mountains. Quart J Roy Meteor Soc 1949; 75: 41–56
- [15]. Romasevich V.F. Helicopter Aerodynamics and Dynamics. Moscow: Voenizdat, 1982.